Supplementary Information

Direct Electrochemical Synthesis of Oxygenates from Ethane using Phosphate-based Electrolysis Cells

Yusuke Honda, Naoya Fujiwara, Shohei Tada, Yasukazu Kobayashi, Shigeo Ted Oyama, and Ryuji Kikuchi*

Department of Chemical System Engineering, School of Engineering,
The University of Tokyo, 7-3-1 Hongo, Bunkyo-ku, Tokyo, 113-8656, Japan

Experimental details

Synthesis of the electrolyte

Cesium dihydrogen phosphate, CsH_2PO_4, was synthesized from Cs_2CO_3 (Wako) and aqueous solution of H_3PO_4 (Sigma-Aldrich, ≥ 85 wt.% in water). The mixed solution composed of stoichiometric ratio of Cs_2CO_3 and H_3PO_4 was dried at 100°C for 24 hours and then calcined for 15 hours at 120°C. Silicon pyrophosphate, SiP_2O_7, was synthesized from SiO_2 (Wako, 99.9%) and aqueous solution of H_3PO_4. The solution composed of stoichiometric ratio of SiO_2 and H_3PO_4 was calcined at 200°C for 3 hours, dried at 100°C for 24 hours, calcined at 120°C for 24 hours and then calcined at 700°C for 3 hours. The obtained CsH_2PO_4 powder and SiP_2O_7 powder were mixed with molar ratio of 1 to 2 because the composite with this ratio has higher proton conductivity than those with the other ratios at 220°C. [S1]

Characterizations

The crystal structures of the CsH_2PO_4 powder and the SiP_2O_7 powder were investigated by X-ray diffraction (XRD, RINT-2700, Rigaku).

The cross-sectional morphologies of the cell before and after the reaction were observed by scanning electron microscopy (SEM, S-4700, Hitachi).

Preparation of the cell and the reactor

The powder mixture was sandwiched by two commercial Pt/C sheets (Miclab, Pt loading 1 mg cm^{-2}, where the Pt/C catalyst was loaded on carbon paper) in a uniaxial pelletizer, and pressed at 13.6 MPa for 10 min to obtain a cell of 10 mm in diameter.

A configuration of a reactor used in the ethane oxidation reaction test is shown in Fig. S5. The prepared cell was set in the center of the reactor. Polytetrafluoroethylene (PTFE) sheets (Gore® Hyper-Sheet® Gasket, W. L. Gore & Associates, Inc.) were used as an insulator and PTFE tapes were used

for gas sealing. Carbon paper in the Pt/C sheets, stainless plates and Pt wire were used to collect current.

Measurement methods

The reactor was heated in a furnace from room temperature to 220°C at the rate of 200°C h^{-1}. When the cell temperature reached 120°C, both the cathode and the anode started to be humidified with 30% of steam in N_2 flow. The both electrodes were reduced in 10 mL min^{-1} H_2 flow under the steam condition for 30 min each before the reaction. The electrochemical reaction test was carried out in a standard gas condition (6% C_2H_6, 30% H_2O and balance N_2 in anode and 30% H_2O and balance N_2 in cathode) with a total flow rate 50 mL min^{-1} each at 220°C at ambient pressure. The electrochemical measurements were conducted using a potentio/galvanostat (Solartron SI 1287) and a frequency response analyzer (Solartron 1255 B) in the two-terminal method. The anode outlet gas composition was analyzed by gas chromatography. The amounts of ethanol and acetaldehyde were analyzed using an on-line gas chromatograph (GC-2014, Shimadzu) equipped with a flame ionization detector (FID) and one type of a column (Porapak Q). The other outlet gas components were analyzed using an on-line gas chromatograph (CP-4900, Varian) equipped with a thermal conductivity detector (TCD) and two types of columns (molecular sieve 5A and Porapak Q).

The effects of the polarization to the oxygenates production were examined by changing the voltage applied to the cell in the following order, open circuit → 10 V → 5 V → 2.5 V → 14 V. The production rates of the products are shown in Fig. S6, and time courses of the current density for the respective applied voltages are present in Fig. S7.

The comparison of two types of oxidizing species (O_2 molecule and surface O species derived from water splitting) was conducted by flowing current or supplying gas O_2. Current density was changed in the following order, 0 mA cm^{-2} → 100 mA cm^{-2} → 50 mA cm^{-2} → 25 mA cm^{-2}. The number of the oxygen atoms derived from water electrolysis was calculated assuming that the faradaic efficiency was 100%. Gaseous O_2 was supplied by flowing 5%O_2/He in an open circuit in the following order, 0 mL min^{-1} → 5 mL min^{-1} → 3 mL min^{-1} → 2 mL min^{-1}. The production rate of the respective products are shown in Fig. S8, and time courses of applied voltage for the applied currents are shown in Fig. S9. The Faradaic efficiency for the respective products are summarized in Tables S2 and S3. Table S2 summarizes the Faradaic efficiency calculated based on the current needed for oxygen atom generation rate, while Table S3 compiles the Faradaic efficiency based on oxygen stoichiometry for the respective products.

A cell with a carbon paper (CP) instead of Pt/C electrode was prepared for a blank test and the blank test was conducted in the standard gas condition. Another blank test without ethane gas was conducted in a gas condition (30% H_2O and balance N_2 in anode and in cathode) with a total flow rate 50 mL min^{-1} each.

To investigate the effect of the concentration of O* under a constant voltage on the reaction, steam

partial pressure in both sides of the cell was varied from the standard condition with applying a constant voltage of 10 V. The steam partial pressure was changed as 30.4 kPa → 20.3 kPa → 40.5 kPa with a constant total flow rate of 50 mL min^{-1}. Ethane flow rate was fixed to 3 mL min^{-1} while N_2 flow rate was changed to achieve the situation. Current densities during the reaction were about 135 mA cm^{-2}, 125 mA cm^{-2} and 200 mA cm^{-2}, respectively. Different current densities correspond to different concentrations of O*. The Faradaic efficiency for the products in this experiment are summarized in Table S4, which was calculated based on current density.

To investigate the effect of the ethane partial pressure under a constant voltage on the reaction, ethane partial pressure in anode side was varied from the standard condition with applying a constant voltage of 10 V. The ethane partial pressure was changed as 10 kPa → 6.1 kPa → 3.0 kPa with a constant total flow rate of 30 mL min^{-1}. Steam partial pressure was fixed to 30 .4 kPa while N_2 flow rate was changed to achieve the situation.

Ethanol oxidation test was performed as follows: ethanol gas was supplied at saturated pressure at 0^oC by bubbling of ethanol with N_2. The gas condition was 1.6% C_2H_5OH and balance N_2 in the anode and 30% H_2O and balance N_2 in the cathode with a total flow rate 50 mL min^{-1} at 220^oC at ambient pressure. The electrochemical measurements were conducted using the same apparatus, and the outlet gases were analyzed by the same method as the case of the ethane oxidation. The measurements were conducted in the following order, 0 mA cm^{-2} → 50 mA cm^{-2} → 25 mA cm^{-2} → 12.5 mA cm^{-2} → 37.5 mA cm^{-2}. In the case of changing applied voltages, the measurements were conducted in the following order, 0 V → 10 V → 2.5 V.

Acetaldehyde oxidation test was performed as follows: acetaldehyde gas was supplied at saturated pressure at 0^oC by bubbling of aqueous solution of acetaldehyde using N_2 gas. The gas condition was 44% CH_3CHO and balance N_2 in the anode with a total flow rate 23 mL min^{-1} and 30% H_2O and balance N_2 in the cathode with a total flow rate 50 mL min^{-1} at 220^oC at ambient pressure. The electrochemical measurements were conducted using the same apparatus, and the outlet gases were analyzed by the same method as the case of the ethane oxidation. The measurements were conducted in the following order, 0 mA cm^{-2} → 50 mA cm^{-2} → 25 mA cm^{-2} → 12.5 mA cm^{-2} → 37.5 mA cm^{-2}.

Calculation of the ethane conversion and the selectivity to the products

The ethane conversion and the selectivity to the products were calculated by the equations below:

$$\text{Ethane conv.} = \frac{F_{CO} + F_{CO_2} + F_{CH_4} + 2F_{C_2H_4} + 2F_{C_2H_5OH} + 2F_{CH_3CHO} + 3F_{C_3H_6} + 3F_{C_3H_6}}{F_{CO} + F_{CO_2} + F_{CH_4} + 2F_{C_2H_4} + 2F_{C_2H_6} + 2F_{C_2H_5OH} + 2F_{CH_3CHO} + 3F_{C_3H_6} + 3F_{C_3H_6}} \quad \text{(S-1)}$$

$$\text{Product}_{C_i}\text{ sel.} = \frac{iF_{C_i}}{F_{CO} + F_{CO_2} + F_{CH_4} + 2F_{C_2H_4} + 2F_{C_2H_5OH} + 2F_{CH_3CHO} + 3F_{C_3H_6} + 3F_{C_3H_6}} \quad \text{(S-2)}$$

where F indicates flow rate of the gas.

Calculation of the value of the kinetic orders for ethane and the O species

The amount of the O species generated from water splitting was assumed to be proportional to the current density flowing through the cell.

The value of α was calculated using the data shown in Fig. S12. The concentration of O* was assumed to be constant:

$$k' = k[O^*]^{\beta} \quad \text{(S-3)}$$

$$r_{CH_3CHO} = k'[C_2H_6]^{\alpha} \quad \text{(S-4)}$$

Taking the natural log of both sides,

$$\ln r_{CH_3CHO} = \ln k' + \alpha \ln [C_2H_6] \quad \text{(S-5)}$$

$\ln r_{CH_3CHO}$ was plotted against $\ln [C_2H_6]$. The value of α was calculated from the slope of the curve and it was 0.31.

The value of β was calculated using the data shown in Fig. S11. the ethane concentration was assumed to be constant:

$$k'' = k[C_2H_6]^{\alpha} \quad \text{(S-6)}$$

$$r_{CH_3CHO} = k''[O^*]^{\beta} \quad \text{(S-7)}$$

Taking the natural log of both sides,

$$\ln r_{CH_3CHO} = \ln k'' + \beta \ln [O^*] \quad \text{(S-8)}$$

$\ln r_{CH_3CHO}$ was plotted against $\ln [O^*]$. The value of β was calculated from the slope of the curve and it was 1.6.

Explanation for the meaning of the kinetic order for ethane partial pressure

It was assumed that ethane was converted to products through the following adsorption steps:

$$C_2H_6 + V_a \overset{k_1}{\rightarrow} C_2H_6\,(ads) \tag{S-9}$$

$$C_2H_6\,(ads) \overset{k_2}{\rightarrow} P \tag{S-10}$$

where C_2H_6, V_a, $C_2H_6\,(ads)$, P, k_1 and k_2 indicate a gaseous ethane molecule, a vacant adsorption site on the catalyst surface, an adsorbed ethane species, the product derived from ethane, a rate constant for the adsorption step and a rate constant for the desorption step, respectively.

When the concentration of a substance A is expressed as $[A]$, total concentration of the vacant adsorption sites, $[V_a\,(total)]$, can be written as below:

$$[V_a\,(total)] = [C_2H_6\,(ads)] + [V_a] \tag{S-11}$$

Here, $[V_a\,(total)]$ is considered to be constant.

The generation rate of the absorbed ethane species is expressed as

$$\frac{d[C_2H_6\,(ads)]}{dt} = k_1[C_2H_6][V_a] - k_2[C_2H_6\,(ads)] \tag{S-12}$$

Assuming a steady state,

$$\frac{d[C_2H_6\,(ads)]}{dt} = 0 \tag{S-13}$$

$$[C_2H_6\,(ads)] = \frac{k_1}{k_2}[C_2H_6][V_a] \tag{S-14}$$

From (S-11) and (S-14), it holds that

$$[V_a\,(total)] = [V_a]\left\{1 + \frac{k_1}{k_2}[C_2H_6]\right\} \tag{S-15}$$

The production rate of the product P, r, is represented as below:

$$r = k_2[C_2H_6\,(ads)] = k_1[C_2H_6][V_a] \tag{S-16}$$

Based on (S-15),

$$r = \frac{[V_a\,(total)]k_1[C_2H_6]}{1 + \frac{k_1}{k_2}[C_2H_6]} \tag{S-17}$$

This is a convex upward function of $[C_2H_6]$, and monotonically increases. Therefore, if (S-17) is approximated by an exponential function with a constant, K, and the kinetic order, α (S-18), the value of α should be greater than 0 and less than 1.

$$r = K[C_2H_6]^{\alpha} \tag{S-18}$$

Calculation of the Faradaic efficiency for the products by partial oxidation of ethane

Hydrogen generation at the cathode is expressed as

$$2H^+ + 2e^- \rightarrow H_2 \quad \text{(S-19)}$$

The anodic reaction for H_2O oxidation is assumed to form the oxidative species O* as

$$H_2O \rightarrow O^* + 2H^+ + 2e^- \quad \text{(S-20)}$$

Ethane oxidation reactions at the anode by O* to form CO, CO_2, CH_4, C_2H_4, C_2H_5OH, and CH_3CHO are assumed as

$$C_2H_6 + 2O^* \rightarrow 2CO + 3H_2 \quad \text{(S-21)}$$

$$C_2H_6 + 4O^* \rightarrow 2CO_2 + 3H_2 \quad \text{(S-22)}$$

$$C_2H_6 + O^* + H_2O \rightarrow 2CH_4 + O_2 \quad \text{(S-23)}$$

$$C_2H_6 + O^* \rightarrow C_2H_4 + H_2O \quad \text{(S-24)}$$

$$C_2H_6 + O^* \rightarrow C_2H_5OH \quad \text{(S-25)}$$

$$C_2H_6 + O^* \rightarrow CH_3CHO + H_2 \quad \text{(S-26)}$$

Accordingly, the stoichiometry of the respective products to O* is 1, 2, 0.5, 1, 1, and 1. Provided that O* was generated only by H_2O oxidation at the anode and that O* was used to produce O_2 and the products mentioned above, Faradaic efficiency based on the number of oxygen atoms is defined as

$$Faradaic\ efficiency\ [\%] = \frac{100 \times n_i F_i}{F_{CO} + 2F_{CO_2} + 0.5F_{CH_4} + F_{C_2H_4} + F_{C_2H_5OH} + F_{CH_3CHO} + 2F_{O_2}} \quad \text{(S-27)}$$

where F_i is a molar flow rate of species i, and n_i is the stoichiometry of species i to O*. The stoichiometry for O_2 is 2, as 2O* are used to generate O_2. Faradaic efficiency is also defined based on the number of electrons accompanying O* generation as

$$Faradaic\ efficiency\ [\%] = \frac{100 \times n_i F_i}{iA/(2 \times 96485)} \quad \text{(S-28)}$$

where i and A represent the current density and the electrode area in electrolysis experiments, respectively, and 96485 is the Faraday constant. If the Faradaic efficiency values calculated by Eqns. S-27 and S-28 accord well with each other, all the O* species is consumed to the products generation. In this case, total Faradaic efficiency determined by Eqn. S-29 becomes close to 100%.

$$Total\ Faradaic\ efficiency\ [\%] = \frac{100 \times \sum n_i F_i}{iA/(2 \times 96485)} \quad \text{(S-29)}$$

Table S1 summarizes Faradaic efficiency of O_2 generated in water electrolysis using the electrolysis reactor shown in Fig. S5. The Faradaic efficiency in Table S1 corresponds to the total Faradaic efficiency defined by Eqn. S-29. The theoretical value means that the oxygen flow generated by water

electrolysis with an assumption of 100% Faradaic efficiency, whereas the detected amount is the actual amount of the oxygen from the anode quantified by the gas chromatograph, and was converted to the flow rate.

Table S1. Faradaic efficiency for water splitting calculated based on the amount of O_2.

Current density [mA cm^{-2}]	Theoretical value [mL min^{-1}]	Detected amount [mL min^{-1}]	Faradaic efficiency [%]
50	0.14	0.13	93

Gas condition: 30%H_2O/N_2 in the anode, 30%H_2O/N_2 in the cathode with a total flow rate 50 mL min^{-1} each. Temperature: 220°C.

Tables S2 and S3 summarize Faradaic efficiency for the products by ethane partial oxidation shown in Figs. 2b and S8. The Faradaic efficiency in Table S2 was calculated by Eqn. S-28. The "Total" represents the efficiency determined by Eqn. S-29. The total Faradaic efficiency is ca. 90% for the operation with 25 and 50 mA cm^{-2}, which is very close to the efficiency by the water electrolysis experiment shown in Table S1.

Table S2 Faradaic efficiency determined by electron balance of the products in ethane oxidation with oxygen species generated by water splitting. The experimental results are also shown in Figs. 2b and S8.

Current density [mA cm^{-2}]	Oxygen atom generation rate [μmol s^{-1}]	Faradaic efficiency [%]							
		O_2	CO_2	CO	CH_4	C_2H_4	CH_3CHO	C_2H_5OH	Total
0	0	NA	NA	NA	NA	NA	NA	NA	-
25	0.10	66.4	22.1	0.0	0.0	0.0	0.4	0.0	89.0
50	0.20	71.5	17.6	0.3	0.0	0.1	0.3	0.0	89.8
100	0.41	8.7	71.5	3.7	0.0	0.5	0.2	0.0	84.8

Table S3 summarizes Faradaic efficiency calculated by Eqn. S-27 for the products by ethane partial oxidation in the electrolysis cell. These calculations of the Faradaic efficiency assumed oxygen atom balance, and as the results in Table S2 indicate that the balance is less than 100%, the Faradaic

efficiency values are larger than the corresponding values in Table S2. Nevertheless, the trends in the Faradaic efficiency for the respective products in Table S3 are well accord with those in Table S2.

Table S3 Faradaic efficiency determined by oxygen atom balance of the products in ethane oxidation with oxygen species generated by water splitting. The experimental results are also shown in Figs. 2b and S8.

Current density	Faradaic efficiency [%]						
[mA cm^{-2}]	O_2	CO_2	CO	CH_4	C_2H_4	CH_3CHO	C_2H_5OH
0	NA	NA	NA	NA	NA	NA	NA
25	74.6	24.9	0.0	0.0	0.1	0.5	0.0
50	79.7	19.6	0.3	0.0	0.1	0.4	0.0
100	10.3	84.3	4.4	0.0	0.6	0.3	0.0

Table S4 summarizes Faradaic efficiency calculated by Eqn. S-27 for the products by ethane partial oxidation in the electrolysis cell. The results in Table S4 corresponds to those in Fig. S11 where the effect of water vapor pressure on the ethane partial oxidation was investigated. It is of note that the Faradaic efficiency for acetaldehyde was increased with the partial pressure of water vapor under the large current density of 200 mA cm^{-2} and the high applied voltage of 10 V, the Faradaic efficiency of CO_2 was kept low at 21.7%.

Table S4 Faradaic efficiency for the products in ethane oxidation under different water vapor partial pressures. Experimental conditions are the same as those in Fig. S11. Applied voltage: 10 V

Water vapor pressure [kPa]	Current density [mA cm^{-2}]	Faradaic efficiency [%]						
		O_2	CO_2	CO	CH_4	C_2H_4	CH_3CHO	C_2H_5OH
20.3	135	92.4	5.4	0.7	0.0	0.6	0.9	0.0
30.4	125	78.0	17.5	1.8	0.0	1.5	1.2	0.0
40.5	200	74.0	21.7	0.5	0.8	0.7	2.2	0.1

Table S5 compiles the production rate of the anode products in electrolysis at a current loading of 50 mA cm^{-2} with a carbon paper anode by feeding humidified N_2 (Entry 4 in Table 1) or humidified C_2H_6 + N_2 (Entry 6 in Table 1). In these cases carbon paper was employed as the anode. Without the Pt/C electrode catalyst in the anode, the main product was CO_2 and O_2 irrespective of C_2H_6 in the feed.

This means the Pt/C catalyst is indispensable for C_2H_6 conversion in the electrolysis cell investigated in this study. Oxygen evolution assures steam electrolysis proceeds over the carbon paper anode in the experimental conditions.

Table S5 Production rate of the anode products in electrolysis at 50 mA cm^{-2} with a carbon paper anode. Entry 4 and 6 are the same conditions as in the Table 1. Humidified N_2 without/with C_2H_6 was fed to the carbon paper anode in Entry 4 and 6, respectively.

Entry	Anode	Gas condition (N_2, Steam)	Production rate [10^{-9} mol s^{-1} cm^{-2}]						
			O_2	CO_2	CO	CH_4	C_2H_4	CH_3CHO	C_2H_5OH
4	Carbon	Without C_2H_6	106	108	5.89	0.0	0.0	0.0	0.0
6	paper	With C_2H_6	119	120	6.06	0.0	0.013	0.0	0.0

Table S6 Comparison of the production rates on a catalyst weight basis.

Temperature [°C]	Catalyst	Oxidant	Applied current [mA]	Production rate [μmol g-cat^{-1} s^{-1}]											Ref. No in the main text
				C_2H_4	C_2H_5OH	CH_3CHO	CH_4	CO	CO_2	HCHO	CH_3OH	HCOOH	CH_3COOH	C_2H_5COOH	
80 [a]	Nafion-H	O_2	40	0	0.26	0.54	-	-	-	-	-	-	-	-	14
220 [a]	Pt	H_2O	79 [c]	2.8	0	1.2	0	19.4	185.3	-	0	-	-	-	This work
			160 [d]	5.2	0.42	16	11.3	3.9	79	-	0	-	-	-	
475 [a]	Au	O_2	5.3	0	0	0.16	0	0	0.39	-	-	-	-	-	15
50 [b]	H-LTA-Pt [e]	H_2O_2	-	-	0.0097	-	-	-	-	-	0.0062	0.00071	0.0022	-	10
100 [b]	Ir_n/ND[g]	O_2	-	0.0064	0.063	0.2	-	-	-	-	0.0041	-	0.12	0.023	8
400 [b]	$FePO_4$	N_2O	-	1.4	0.23	0.47	-	0.29	0.29	0.14	-	-	-	-	11
550 [b]	B/BPO_4	O_2	-	0.26	-	0.84	-	0.31	0.06	0.12	-	-	-	-	12
650 [b]	V_2O_5/O-dia [f]	CO_2	-	0.50	-	0.039	-	-	-	0.0053	-	-	-	-	13

[a] Electrochemically. [b] Thermal catalytically. [c] 30% steam condition applying 100 mA cm^{-2}. [d] 40% steam condition applying 10 V. [e] Pt containing LTA zeolite. [f] V_2O_5 supported on oxidized diamond. [g] Iridium cluster on nano-diamond.

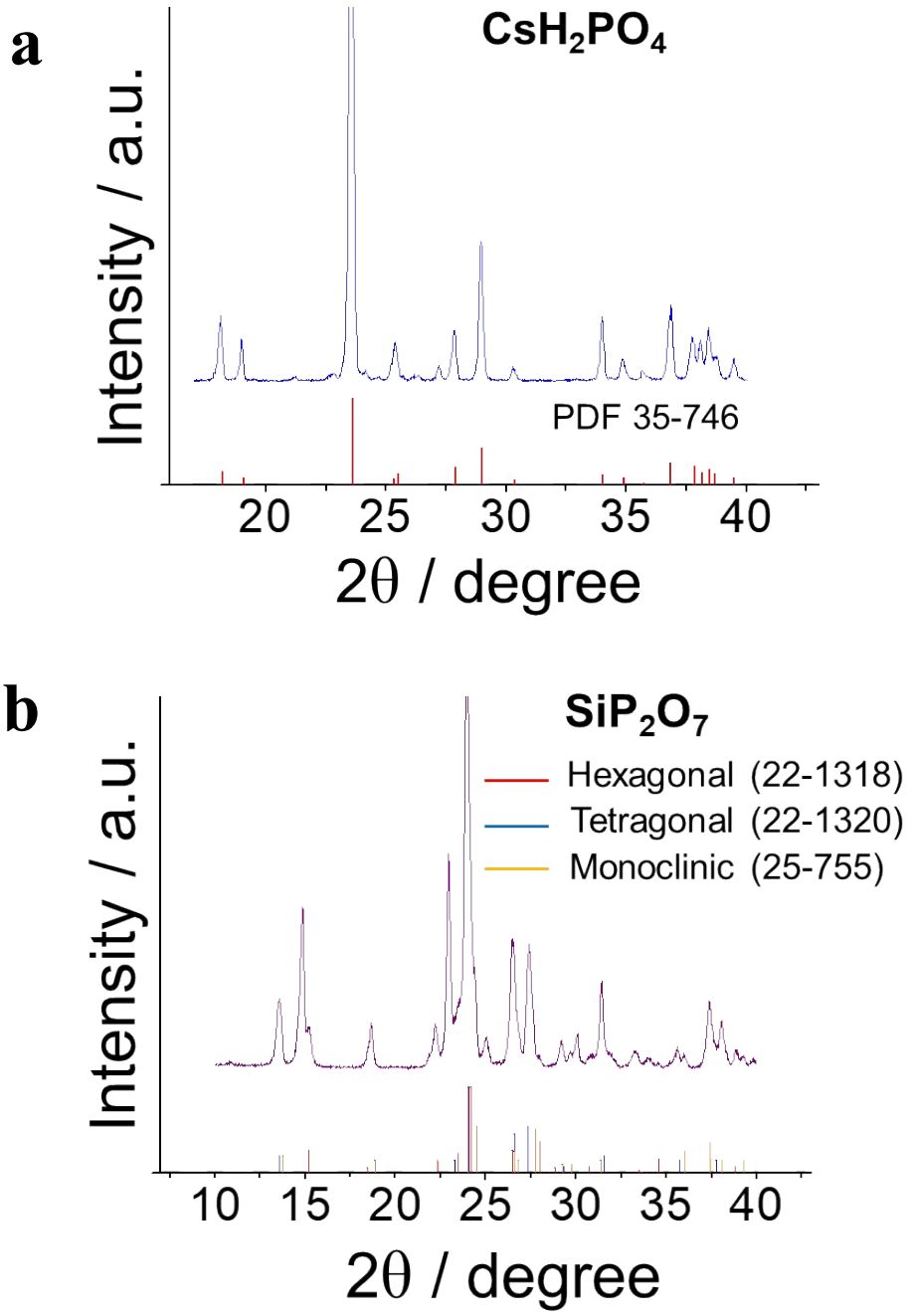

Figure S1. XRD patterns for a) CsH_2PO_4 powder and b) SiP_2O_7 powder.

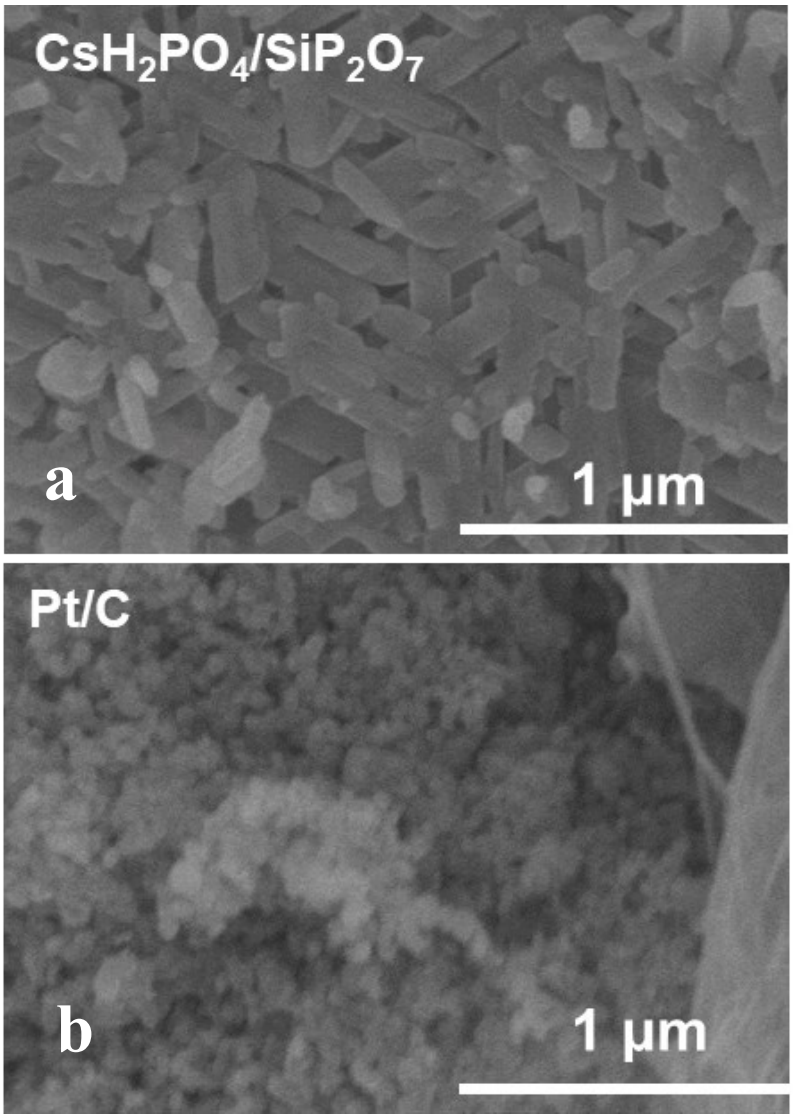

Figure S2. SEM images of a) electrolyte composite and b) Pt/C catalyst before the ethane oxidation test.

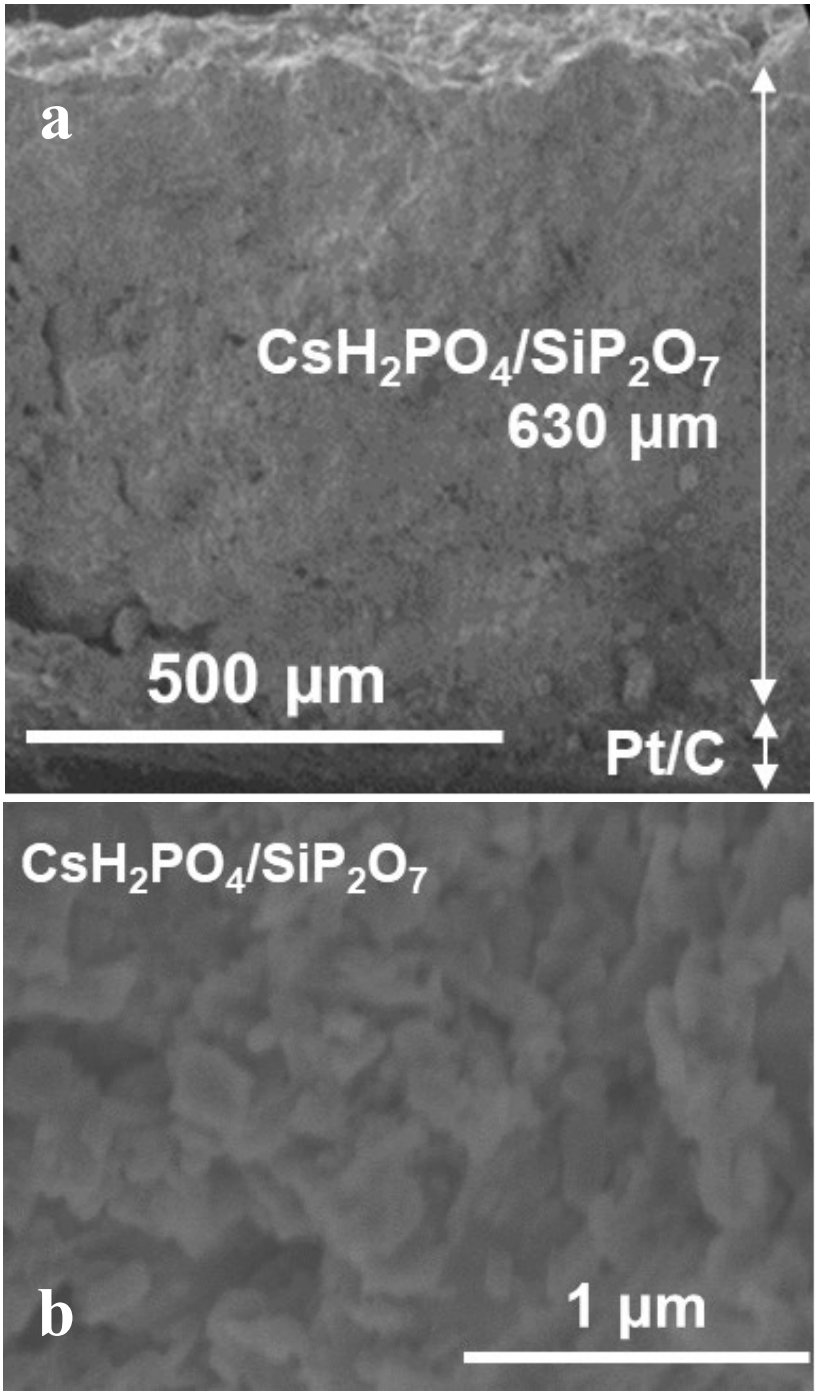

Figure S3. SEM images of a) the cell and b) the electrolyte composite after the ethane oxidation test.

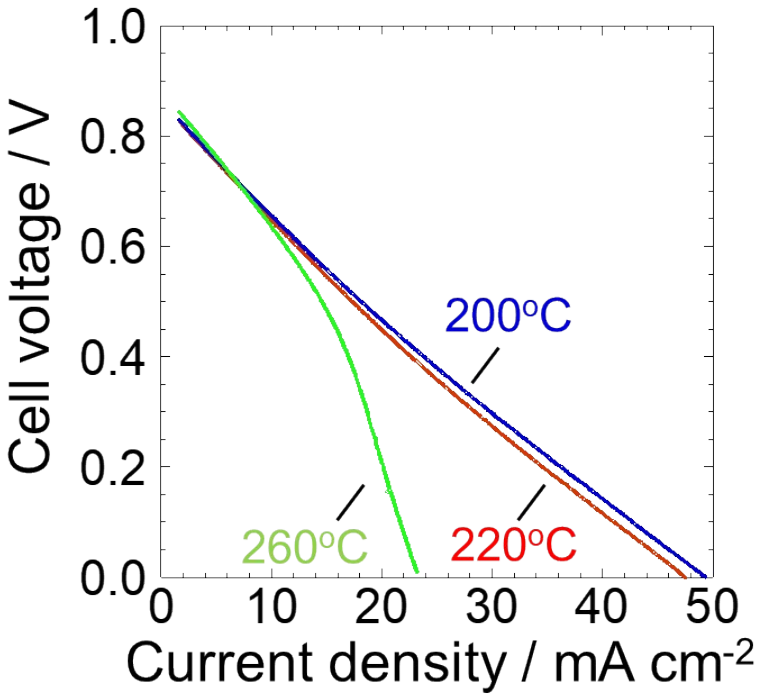

Figure S4. I-V test at several temperatures. Gas condition: 30%H_2O/H_2 in the anode, 30%H_2O/O_2 in the cathode with a total flow rate 50 mL min^{-1} each. Scan rate: 5 mV s^{-1}. The electrochemical performance of the cell at 260°C was deteriorated due to the dehydration of the phosphate-based electrolyte.[S1]

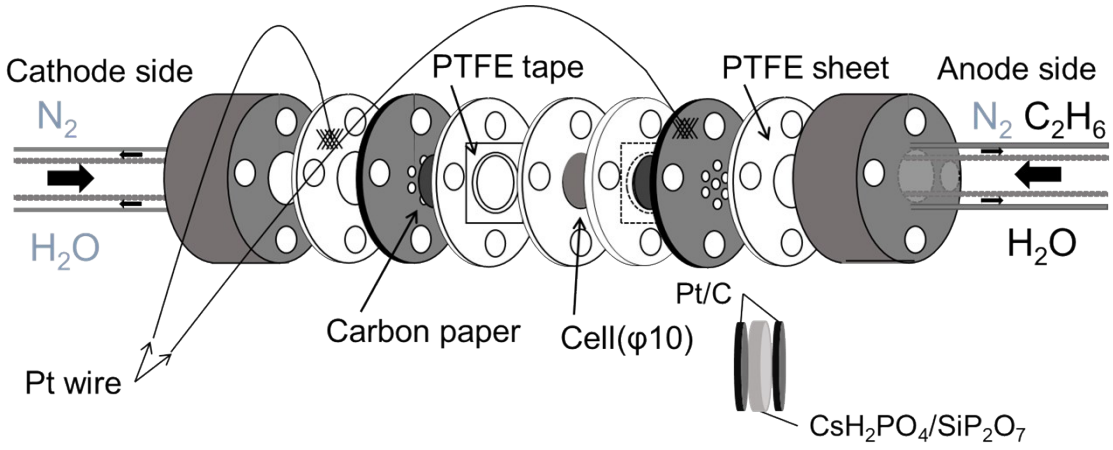

Figure S5. A configuration of a reactor used in the ethane oxidation.

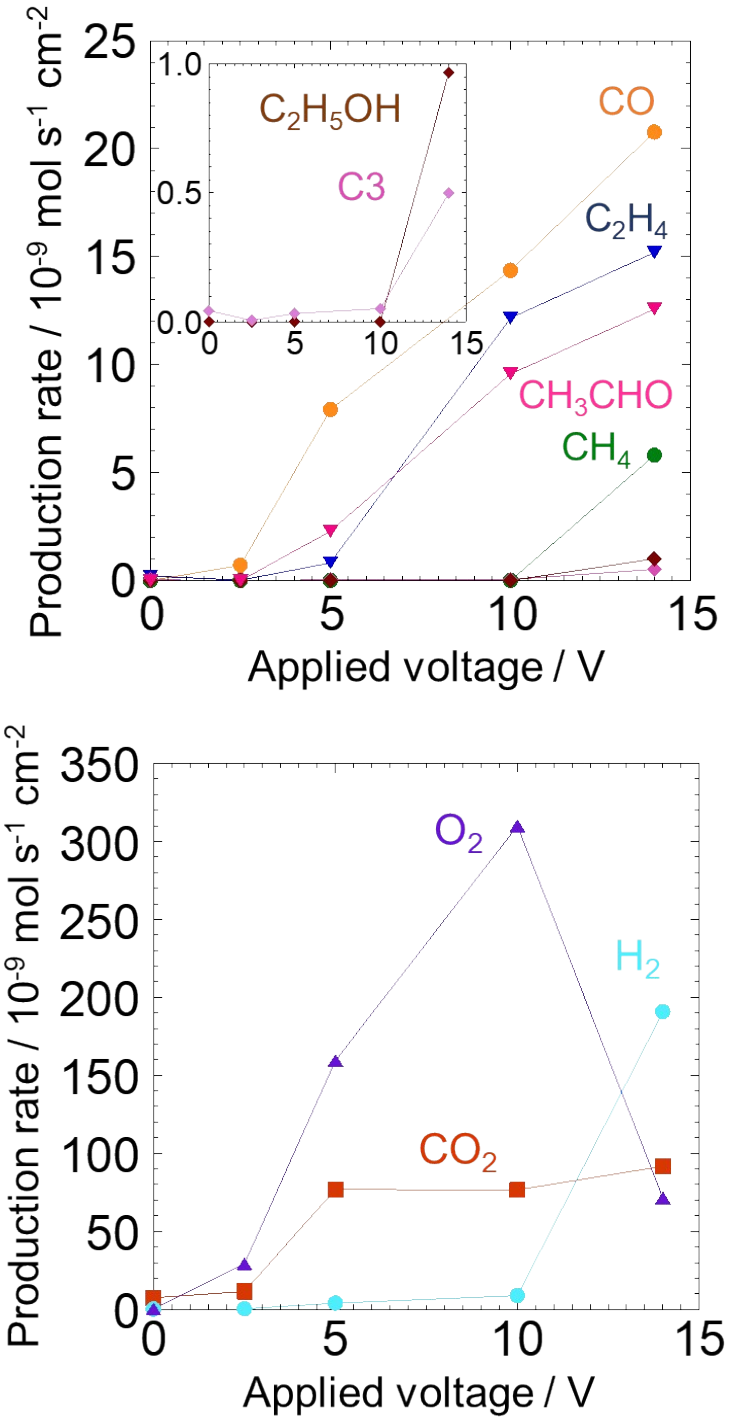

Figure S6. The effect of applied voltage on the production rates of CO, C_2H_4, CH_3CHO, CH_4, C_2H_5OH, C3 species, CO_2, O_2 and H_2.

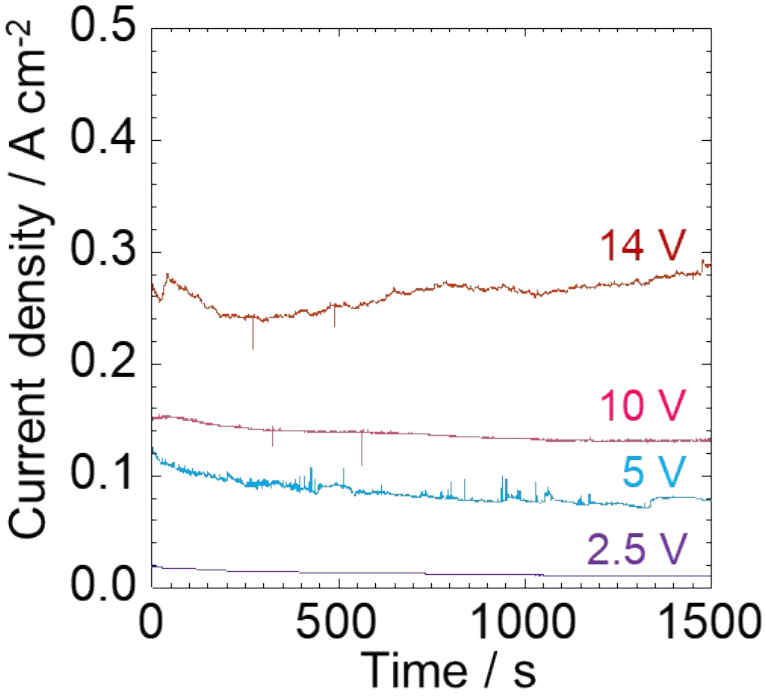

Figure S7. Current densities at different applied voltages during the ethane oxidation test.

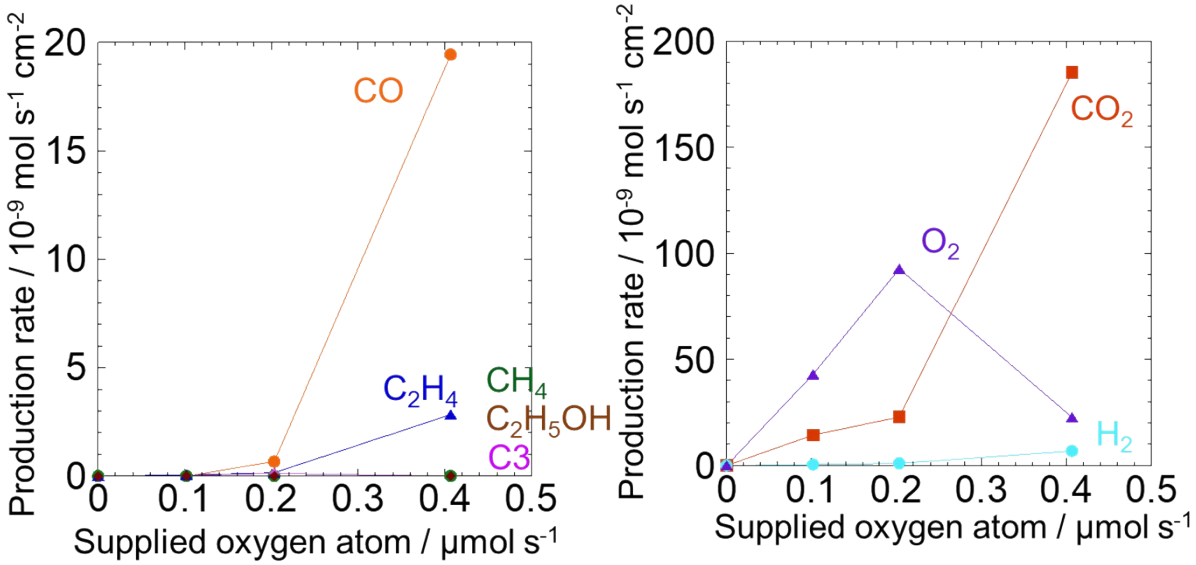

Figure S8. The effect of the amount of supplied oxygen atoms generated by water splitting on the production rates of CO, CH_4, C_2H_4, C_2H_5OH, C3 species, CO_2, O_2 and H_2.

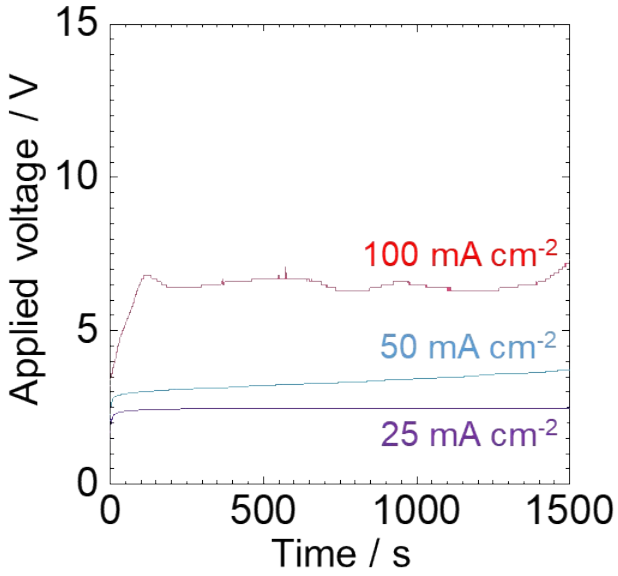

Figure S9. Applied voltages at different current densities during the ethane oxidation test.

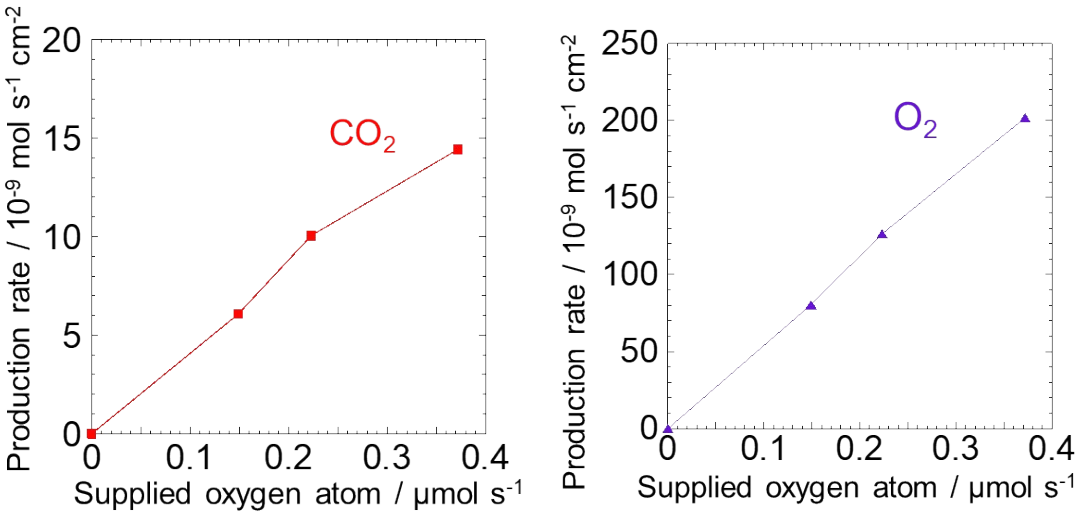

Figure S10. The effect of the amount of oxygen atoms fed as O_2 gas on the production rates of CO_2 and O_2. The selectivity to CO_2 was 100 % in the presence of O_2 gas.

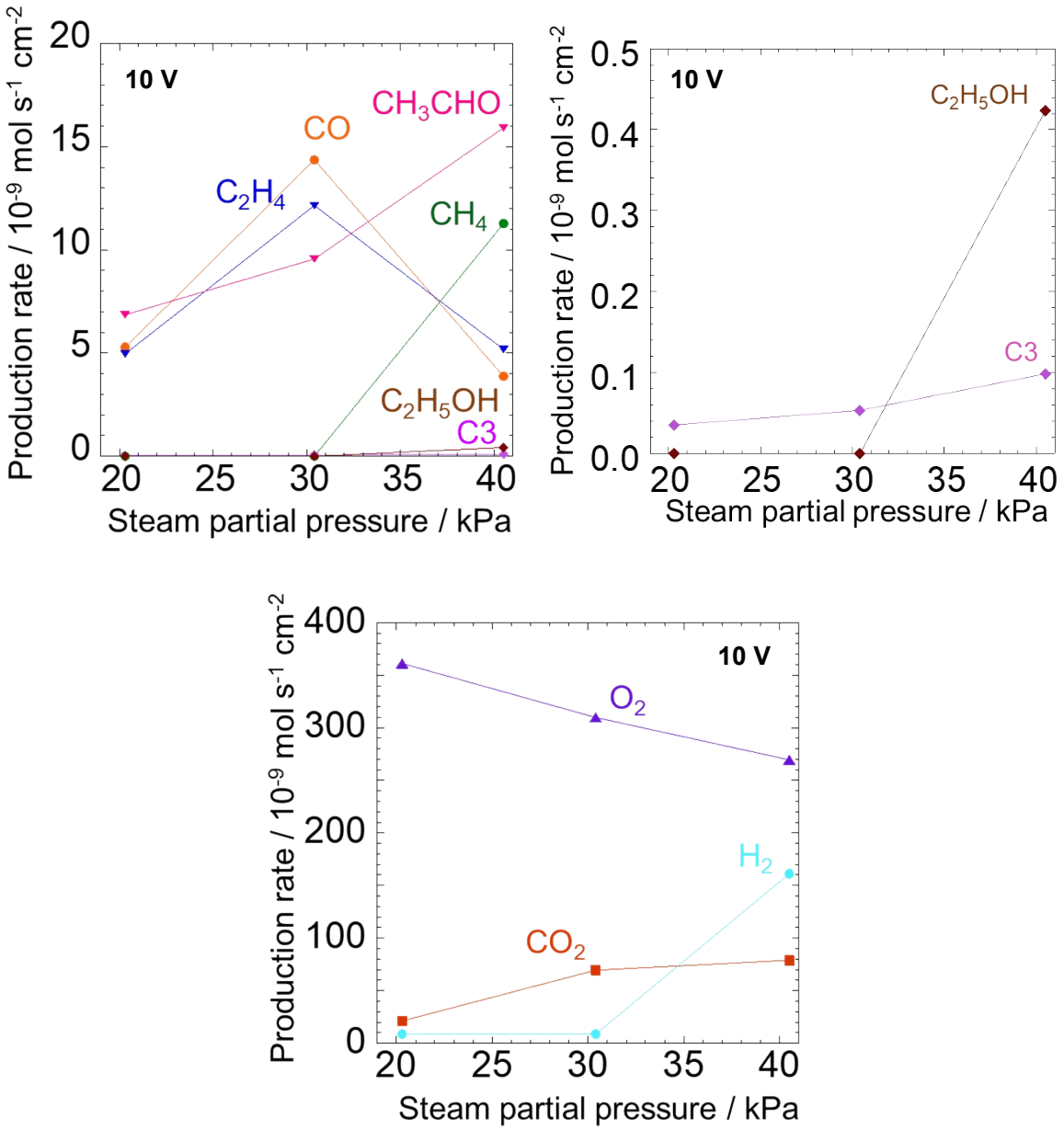

Figure S11. The production rates of CO, CH_4, C_2H_4, CH_3CHO, C_2H_5OH, C3 species, CO_2, O_2 and H_2 obtained under different steam partial pressures and a constant voltage of 10 V. The steam partial pressure was changed as 30.4 kPa → 20.3 kPa → 40.5 kPa with a constant total flow rate of 50 mL min^{-1}. Ethane flow rate was fixed to 3 mL min^{-1} while N_2 flow rate was changed to achieve the situation. Current densities during the reaction were about 135 mA cm^{-2}, 125 mA cm^{-2} and 200 mA cm^{-2}, respectively. Different current densities correspond to different concentrations of O*.

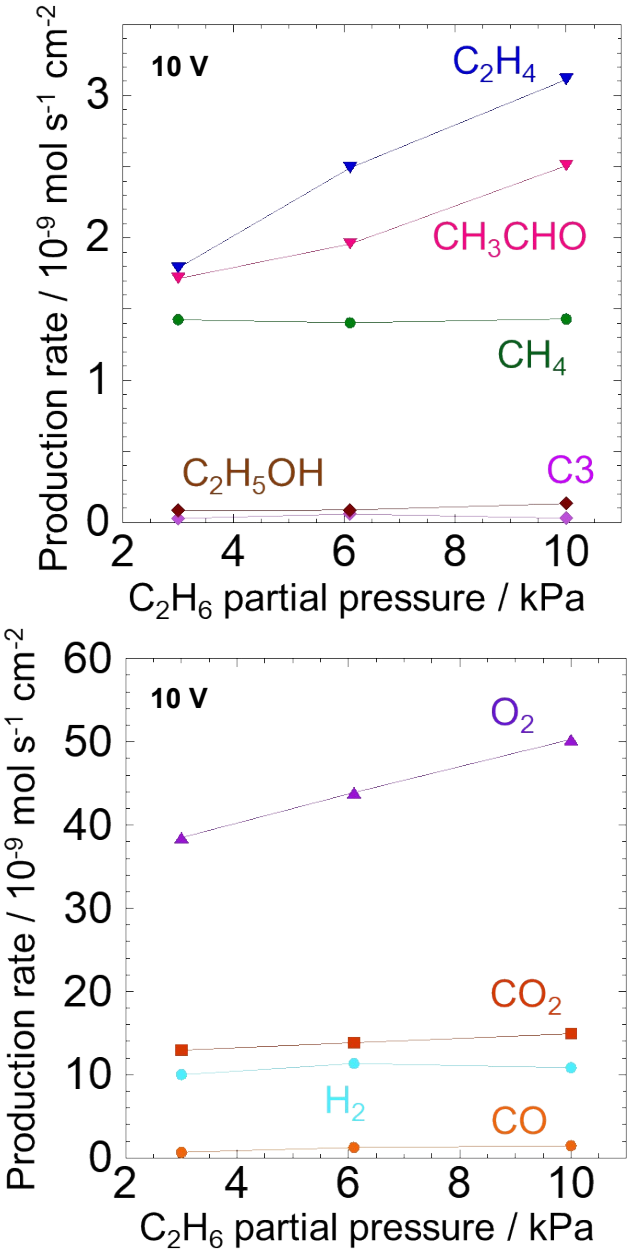

Figure S12. The effect of ethane partial pressure on the production rate of CO, CH_4, C_2H_4, CH_3CHO, C_2H_5OH, C3 species, CO_2, O_2 and H_2 under a constant voltage of 10 V. The ethane partial pressure was changed as 10 kPa → 6.1 kPa → 3.0 kPa with a constant total flow rate of 30 mL min^{-1}. Steam partial pressure was fixed to 30 % while N_2 flow rate was changed to achieve the situation. The current densities during this test were almost constant, 40 mA cm^{-2}, regardless of the ethane partial pressure.

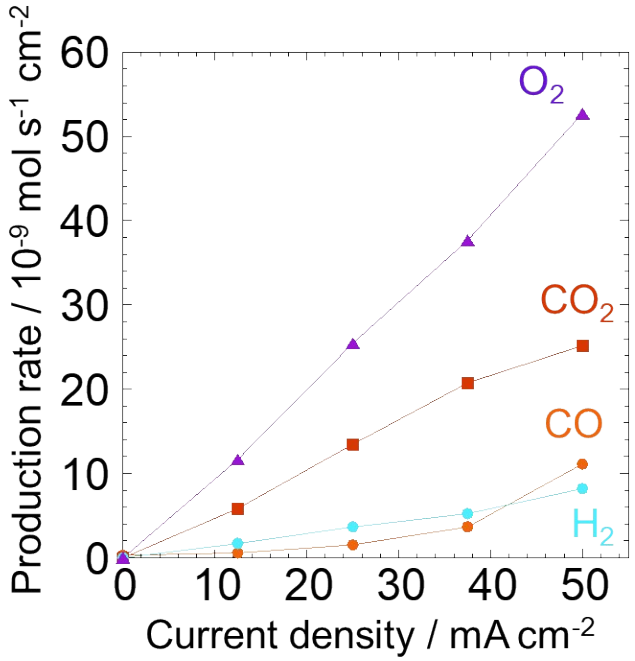

Figure S13. Ethanol oxidation test. The production rate of CO, CO_2, O_2 and H_2 at different current densities.

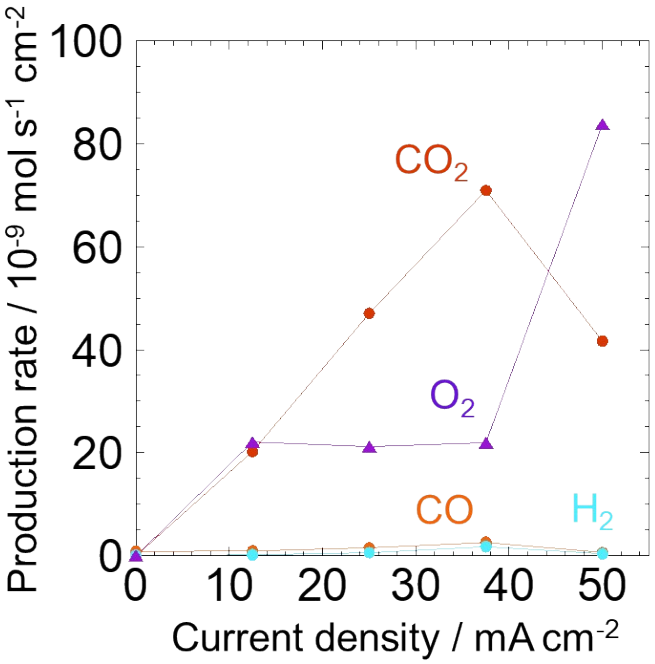

Figure S14. Acetaldehyde oxidation test. The production rate of CO, CO_2, O_2 and H_2 at different current densities.

S1 T. Matsui, T. Kukino, R. Kikuchi, K. Eguchi, *J. Electrochem. Soc.*, 2006, **153**, A339-A342.